

Universality and Deposition Morphology of Granular Column Collapses

Teng Man^{1,2,*}, Herbert E. Huppert^{3,†}, Ling Li^{2,‡} and Sergio Andres Galindo-Torres^{2§}

¹*Institute of Advanced Technology, Westlake Institute for Advanced Study,
18 Shilongshan St., Hangzhou 310024, Zhejiang Province, China*

²*School of Engineering, Westlake University, 18 Shilongshan St., Hangzhou, Zhejiang 310024, China and*

³*Institute of Theoretical Geophysics, King's College, University of Cambridge,
King's Parade, Cambridge CB2 1ST, United Kingdom*

(Dated: December 21, 2024)

The collapse of dry granular materials results in various flow phenomena and deposition morphologies, which we here link to the inter-granular and particle-boundary frictional coefficients and the initial aspect ratio of the granular columns. With the guidance of experiments, computational studies with the discrete element method (DEM) were performed to investigate the universality of dry granular column collapses. The resulting morphology of a collapsed granular column can be linked to an effective initial aspect ratio, and be described by different collapsing regimes, which are controlled by both the effective aspect ratio and the particle-boundary friction. The finding is important for understanding how granular materials, such as debris flows and landslides, behave and how they deposit when the granular flow halts.

Usage: Secondary publications and information retrieval purposes.

PACS numbers:

Structure: You may use the `description` environment to structure your abstract

Introduction.—Granular materials are used widely and encountered frequently in a variety of areas including civil engineering, geophysics, pharmaceutical engineering, and chemical engineering. They can behave like a solid, a fluid, or a gas in different circumstances [1]. In recent decades, with rigorous investigations, breakthroughs have been made to understand the basic governing principles, especially the constitutive relationship, of granular materials. Among these investigations, the proposal of the $\mu(I)$ rheology [2] and the $\mu(I, I_v)$ relationship [3, 4] of granular materials opened a window for exploring the behavior of dense granular materials from a viewpoint of a competition among acting stresses, viscous stresses and inertial stresses [3, 5] (or a competition among different time scales: $1/\dot{\gamma}$, $d/\sqrt{\sigma_n/\rho_p}$, and η_f/σ_n [6], where $\dot{\gamma}$ is the shear rate, σ_n the pressure, ρ_p the particle density, d is the average particle radius, and η_f the viscosity of the interstitial fluid).

The collapse of granular columns drew continuous attention due to the potential link to the dynamics or deposition morphology of geophysical flows [7, 8]. Progress has been made, even though no universal relationship describing the collapse behavior of granular columns has been concluded. Difficulties arise because such systems are highly dependent on inter-particle friction [9] and boundary conditions [8, 11, 12], which was not fully captured by the rheological models previously mentioned. Rigorous investigations [7, 13, 14] have been conducted to understand the behavior of the granular column collapse. Lube et al. [7, 13] and Lajeunesse et al. [14] independently determined that the normalized run-out distance, as well as the halt time, of a collapsed granular column scales with the initial aspect ratio of the column, a parameter drawn out of dimensional analysis. Lube et

al. [13] further concluded that the inter-particle friction only plays an important role in the last instant of the flow when the collapse starts to halt. Staron and Hinch [9] studied the effect of grain properties on the collapse of granular columns and suggested that the frictional coefficient could have an impact on the run-out distance and final mass distribution along the radius. Kermani et al. [16] used the discrete element method (DEM) to investigate the relationship between deposition morphology and inter-particle rotational resistance as well as the initial porosity of the granular packing, based on which they linked the deposition morphology to the energy dissipation.

However, the previous research often lacked physical interpretation of the scaling parameter, i.e. the initial aspect ratio α (which was derived from dimensional analysis [13]), and the universality in the transition point between $\mathcal{R} \propto \alpha$ and $\mathcal{R} \propto \alpha^{1/2}$, where \mathcal{R} is the normalized radial run-out distance [7, 13]. Furthermore, previous studies did not take the inter-granular friction and boundary conditions into consideration. In this letter, with the assistance of both experiments and DEM simulations, we aim to further explore the scaling of the final run-out distance of collapsed granular columns, and link the scaling law with a theoretically derived dimensionless number. The deposition morphology and the correlation between initial height and deposition distance are carefully analyzed. With this work, the regime change of the granular column collapse can be obtained for further investigation of geophysical flows, such as debris flows and landslides.

Simulations and Experiments.— In this study, we performed simulations with DEM [20], which allow us to extract particle-scale data of the system. The simula-

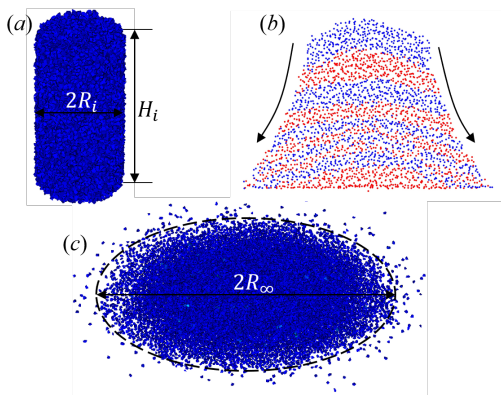


FIG. 1. The initial, intermediate, and final DEM simulations of granular column collapse. Different colors in Fig. 1(b) represent different layers in the initial state.

tions were performed with particles generated from a 3D Voronoi diagram (particle size ≈ 2 mm, Fig. 1). We implemented a simple contact model (presented in the supplemental material) to calculate the interactions among particles. The properties of the particles were set to be the same as that of quartz sand. At the initiation of each simulation, particles were released from a column with diameter of 50 mm. We varied the initial aspect ratio, α , from 0.4 to 20 ($\alpha = H_i/R_i$, where H_i is the initial height of the column and R_i is the radius of the initial holding cylinder). We also varied the inter-particle frictional coefficient, μ_p , from 0.1 to 0.8 and the particle-boundary frictional coefficient, μ_w , from 0.2 to 0.6. Based on these simulations we obtained the run-out behavior and deposition morphology with respect to different conditions. Additionally, in the supplemental material, we present another set of simulations and corresponding experiments for the purpose of validating the DEM model.

Results.—Figure 2(a) - (c) show relationships between the run-out distance and the initial aspect ratio of granular columns with circular cross-sections. It shows that both the inter-particle and particle-boundary frictional coefficients play important roles in the run-out behavior. Generally, when the initial aspect ratio, α is small enough, the normalized run-out distance, $\mathcal{R} = (R_\infty - R_i)/R_i$ where R_∞ is the final run-out radius, scales proportional to α . When α is larger than a threshold value, \mathcal{R} scales proportional to $\alpha^{1/2}$. In each of the figures, as we increase the inter-particle frictional coefficient, the run-out distance decreases since the additional friction increases the energy dissipation during the collapse. Similarly, as we increase the particle-boundary frictional coefficient, the run-out distance also decreases. The influence of inter-particle and particle-boundary frictional coefficients on the flowing behavior of collapsed granular columns was absent in previous studies.

To reveal the deposition morphology, we plot in Fig. 3(a)-(d) the deposition shape of collapsed granular

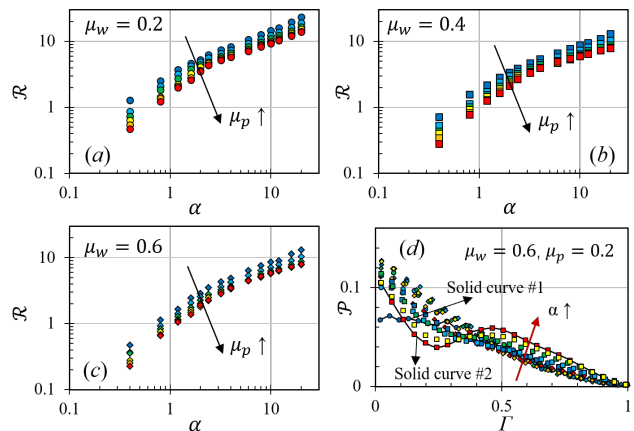


FIG. 2. (a) - (c) show the relationship between normalized run-out distance, \mathcal{R} , and the initial aspect ratio, α , with particle-boundary frictional coefficient equal to 0.2 (circle markers), 0.4 (square markers), 0.6 (diamonds), respectively. Different color represents different inter-particle frictional coefficients. In Fig. (a), \bullet : $\mu_p = 0.1$, \circ : $\mu_p = 0.2$, \diamond : $\mu_p = 0.3$, \square : $\mu_p = 0.4$, \triangle : $\mu_p = 0.6$, \star : $\mu_p = 0.8$. (d) shows the normalized histogram of number of particles, $\mathcal{P} = N(\Delta r)/(rN_p)$, presented at normalized position, $\Gamma = r/R_\infty$ for simulations with $\mu_w = 0.6$ and $\mu_p = 0.2$. In (d), different markers denote results presenting different types of deposition morphologies. \circ are cases where a plateau is formed on top of the deposition, and most particles remain stationary during the collapse, \diamond are cases where top particles tend to flow to the front, and \square are cases where top particles tend to push lower particle outwards. Different colors mean different initial aspect ratios. The solid curves #1 and #2 in Fig. (d) represent numerical simulation results of the shortest and tallest granular column.

columns and the change of deposition shape with respect to the change of the initial aspect ratio. In these figures, we also distinguish particles initially located on the top of the column (blue dots) from the rest (red dots). The results show three different types of deposition morphology. When α is small [Fig. 3(a) and (b)], there is a plateau on top of the granular pile, and blue dots all present on top of red dots. In these cases, a large portion of particles remain stationary during the collapse process, and the granular collapse behaves more like a yielded solid. Thus, we name it the quasi-static collapse. As we increase the initial aspect ratio [Fig. 3(c)], more particles flow down and spread out from the top of the column. In these cases, top particles tend to rest at the foot of the final granular file, and during the collapse, surface granular flows (granular avalanches) dominate the behavior of the granular collapse. The final deposition morphology is similar to a typical sand pile. Thus, we name this type the granular collapse. As we further increase α , the deposition surface changes to Fig. 3(d). Particles initially on the top end up being in the center of the final granular pile, indicating that during the granular collapse, the top particles are flowing downward while pushing the lower

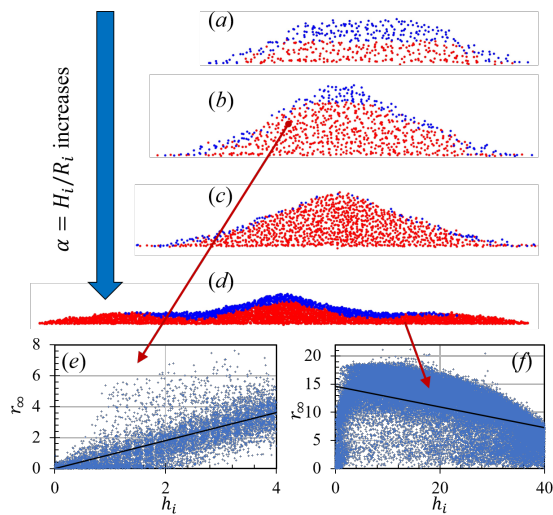


FIG. 3. (a) - (d) Deposition morphology of collapsed granular columns. Blue dots denote particles originally at the top 25% of the column, while red dots represent the rest. (e) and (f) shows the relationship between the initial height and the final radial deposition of each particle. The unit of the axes is centimeters

particles out. We call this type of granular collapse a fluid-like collapse.

We can clearly see these three types of granular collapse in Fig. 2(d), where we plotted the normalized histogram of the number of particles, $\mathcal{P} = N(\Delta r)/(rN_p)$, against the normalized radius, $\Gamma = r/R_\infty$, of the final pile, where $N(\Delta r)$ is the number of particles within a circular bin of width Δr , r is the position where we measure the number of particles, and N_p is the total number of particles of the system. The number probability is normalized with the radius where we take the measurements. This plot is equivalent to the axisymmetric morphology of the final deposition. With the change of initial aspect ratio, α , morphological patterns change accordingly. When α is small the $\mathcal{P}(\Gamma)$ curve starts at a plateau, stays there for a while, and then begins to decrease continuously to 0. This indicates that not all top-layer particles fall down the granular pile when the aspect ratio is smaller than the internal frictional angle [13]. As we increase α , the corresponding $\mathcal{P}(\Gamma)$ curve starts to decrease at the beginning ($\Gamma = 0$), and $\partial\mathcal{P}/\partial\Gamma$ is a monotonically increasing function. With further increase of α , the morphology of the deposited materials changes dramatically. In this case, $\partial\mathcal{P}/\partial\Gamma$ is no longer a monotonic function (solid curve #2 in Fig. 2(d)). We can also see this transition in the plot of the relationship between the initial height and final radial position of each particle [Fig. 3(e) and (f)]. When α is small [Fig. 3(e)], particles initially on the top tend to collapse to the front. Thus, two parameters have a positive correlation in this case. When α is large [Fig. 3(f)], particles initially on

the top no longer reach the front of the final deposition. Thus, the two parameters have a negative correlation.

As we have stated, these three different morphologies correspond to three different collapsing regimes: (1) a quasi-static regime, where most of the bulk material remains relatively stationary, and a plateau can form after the granular collapse; (2) a granular regime, where particles initially at the top end up flowing to the front of the final granular pile; (3) a fluid-like regime, where the collapsed granular materials flow like a fluid to form a much more complex morphology, where particles initially at lower height start to accumulate at the front of the flow due to the push-out effect from particles with larger initial height.

Discussion.—Previous research argued that the run-out distance of a collapsed dry granular column is controlled mainly by the initial aspect ratio with some small influence of the friction. In this letter, the authors propose that the collapse of a granular column and the deposition of it is controlled by the ratio between inertial stresses and the frictional effects. According to Bagnold [21, 22], in a dry granular flow, the inertial stresses scale with $\rho_p \dot{\gamma}^2 d^2$, where he took the distance between adjacent particles in the flowing (or shearing) direction as the characteristic length scale. We interpret $\dot{\gamma}$ as a rate change of unit deformation, and d as a length scale in the flowing direction. In our case, we simplify $\dot{\gamma}$ as $\sqrt{gH_i}/R_i$, which is the ratio between a characteristic velocity when particles fall over the length of H_i and the length scale, R_i , over which the deformation occurs. Meanwhile, d is replaced with H_i , the inertial stresses and thereby $\sigma_i = \rho_p (gH_i/R_i^2) H_i^2$. Additionally, the stresses due to friction can be calculated as $\sigma_f = \mu \sigma_n \propto \mu \phi_s \rho_p g H_i$, where ϕ_s is the solid fraction at the initial state. Thus the ratio between the two stresses can be obtained as

$$\frac{\sigma_i}{\sigma_f} \propto \frac{\rho_p (gH_i/R_i^2) H_i^2}{\mu \phi_s \rho_p g H_i} = \frac{1}{\mu \phi_s} \left(\frac{H_i}{R_i} \right)^2, \quad (1)$$

where μ is a general frictional coefficient, which we take as a linear combination of the inter-particle frictional coefficient and the particle-boundary frictional coefficient, $\mu = \mu_p + \beta \mu_w$. The square root of this formula can be seen as an effective aspect ratio.

$$\alpha_{\text{eff}} = \sqrt{\frac{1}{(\mu_p + \beta \mu_w) \phi_s}} \left(\frac{H_i}{R_i} \right). \quad (2)$$

In our simulations of the collapse of Voronoi packing granular columns, the initial solid fraction of the columns is the same for every case, and $\beta = 0.5$ best fits the simulation data. Fig. 4(a) shows the relationship between \mathcal{R} and α_{eff} . With $\beta = 0.5$, simulation results with $\mu_w = 0.4$ and $\mu_w = 0.6$ collapse onto one curve. Meanwhile, although simulation results with $\mu_w = 0.2$ do not collapse with that of other particle-boundary frictions, the results in this set of simulations can still collapse to one curve

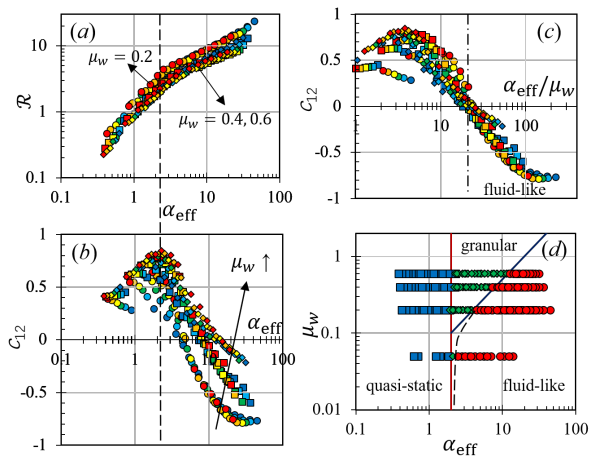


FIG. 4. (a) shows the relationship between \mathcal{R} and the effective aspect ratio that we propose, $\alpha_e = (\sqrt{1/(\mu_p + \beta\mu_w)})(H_i/R_i)$. We see that for data with $\mu_w = 0.4$ and 0.6 , all the data collapse, but the runout distance of $\mu_w = 0.2$ is obviously larger than that in other cases. In (b), the y -axis represents correlation coefficients between the initial height of particles and run-out distances of them, c_{12} , and the x -axis shows the effective aspect ratio of granular columns, α_e . (c) shows the relationship between c_{12} and $\alpha_{\text{eff}}/\mu_w$. The markers represent the same meaning as that in Fig. 2(a)-(c). (d) represents a "phase diagram" of the collapse of granular columns

themselves. Different from previous studies where α is the only criterion to indicate a regime change of the granular column collapse [where the slope of $\mathcal{R}(\alpha)$ changes], we found that, in Fig. 4(a), the slope change in the $\mathcal{R}(\alpha)$ relationship collapsed at one single value of α_{eff} . This indicates that the normalized run-out distance is almost entirely controlled by the effective aspect ratio, α_{eff} , which includes the influence of both inter-particle and particle-boundary frictional coefficients, rather than the initial aspect ratio, α , alone. The reason why run-out distances for $\mu_w = 0.2$ deviate from other cases is that under low particle-boundary friction conditions, more slip occurs when particles collide with the boundary. In other cases, particles have a no-slip boundary condition, where the kinetic energy of particles can be quickly dissipated. In the future, particle-scale contact forces between particles and the boundary should be particularly investigated to verify this hypothesis.

Figure 4(a) shows that the collapse of granular columns clearly has two separate regimes on the basis of the value of α_{eff} . However, according to the analysis of the deposition morphology, these granular flows should have three different regimes. To better investigate these regimes in connection to the deposition morphology, we propose to analyze the relationship between the initial height, h_i , and the final radial position, r_∞ (or the run-out distance, $r_\infty - r_i$) of each particle. Such a relationship can help us better understand how particles end up being at different positions. The correlation coefficient between h_i and

$r_\infty - r_i$ can then be obtained as

$$c_{12} = \frac{\text{cov}[h_i, (r_\infty - r_i)]}{\sigma_h \sigma_r}, \quad (3)$$

where c_{12} is the correlation coefficient between run-out distances and initial heights of particles in a collapsed granular column, $\text{cov}[\]$ is the covariance function, h_i is the initial height of each particle, r_∞ is the final radial position of each particle, r_i is the initial radial position vector, σ_h is the standard deviation of all the initial height data in one system, and σ_r is the standard deviation of all the run-out distances of particles in one system. When c_{12} is positive, more particles initially at the top of a granular column end up at the foot of the deposited pile, whereas when c_{12} is negative, more particles initially at the top cannot even reach the foot and more frequently end at the interior of the deposited granular packing, in which case, the collapse of granular columns behaves more like a fluid where top layer particles push the bottom layer particles away as they fall downward.

Figure 4(b) plots the relationship between c_{12} and α_{eff} . Both frictional coefficient and α_{eff} have great influence on how the correlation coefficient evolves. When α_{eff} is small, c_{12} is positive, and in this case, as we increase α_{eff} , c_{12} increases accordingly and eventually reaches a maximum, which corresponds to the turning point in the $\mathcal{R} - \alpha_{\text{eff}}$ relationship in Fig. 4(a). The α_{eff} which corresponds to the maxima of c_{12} is a threshold which divides the quasi-static collapse and the granular-type collapse. When α_{eff} is larger than this threshold, c_{12} starts to decrease, and at a certain point, it becomes negative, where the collapse of a granular column is in the fluid-like regime.

However, the point when systems change from a granular regime to a fluid-like regime depends not only on α_{eff} but also on other factors, as shown in Fig. 4(b), where the crossing point of $c_{12}(\alpha_{\text{eff}})$ is different for cases with different μ_w . Interestingly, if we plot c_{12} against $\alpha_{\text{eff}}/\mu_w$ instead [Fig. 4(c)], the place where c_{12} passes zero collapses onto one point, $\alpha_{\text{eff}}/\mu_w \approx 20$, which means that the transition from a granular regime to a fluid-like regime depends on $\alpha_{\text{eff}}/\mu_w$. Based on these analyses, a phase diagram of the collapse of granular columns can be obtained and sketched as Fig. 4(d), where the deposition morphology of a collapsed granular column depends on both μ_w and $\alpha_{\text{eff}} = \sqrt{1/[\phi_s(\mu_p + 0.5\mu_w)]}(H_i/R_i)$. More specifically, the transition between quasi-static collapse and granular collapse or fluid-like collapse depends only on the effective aspect ratio, α_{eff} . In contrast, the transition between the granular regime and the fluid-like regime depends on the ratio between α_{eff} and μ_w .

We also performed simulations with $\mu_w = 0.05$, and expected a direct change from quasi-static collapsing to fluid-like collapsing. However, there is still one case showing granular column collapse in the granular regime. Thus, we suspect that, when α_{eff} is approaching $\alpha_{\text{eff}} = 2$,

the regime change between a granular regime and a fluid-like regime should follow the dashed curve in Fig. 4(d). It should also be noted that, since our definition of α_{eff} includes the packing solid fraction, it can be potentially useful in describing the behavior of granular column collapse with different initial packing fractions. Details of the influence of packing fraction will be further investigated in the future.

Summary.—In this letter, we analyzed the scaling of the run-out distance and deposition morphology of collapsed granular columns with respect to the aspect ratio based on numerical simulations using DEM. A dimensionless number, which is derived from the ratio between inertial stresses and friction-induced stresses and includes influences of the frictional coefficient (inter-particle and particle-boundary), the initial aspect ratio, and initial solid fraction, is proposed. Based on the correlation between the initial position and final position of particles, we further divide the collapse of granular columns into three regimes (quasi-static, granular, and fluid-like), which are controlled by both α_{eff} and μ_w . This study shows that the boundary friction can be crucial to the final deposition of a collapsed granular column, which can bring insight to the behavior of landslides or debris flows in future studies. Additionally, the introduction of the solid fraction in α_{eff} , although it plays no role in this study, could bring opportunities to understand better in coming studies how the initial packing of granular materials influences the collapsing dynamics of granular materials in both sub-aerial and sub-aqueous environment.

The authors acknowledge the financial support from Westlake University, and thank the Westlake University Supercomputer Center for computational resource and related assistance. T. M. would like to thank Prof. K. M. Hill from University of Minnesota for helpful discussions on collapses of granular columns. The authors specifically thank Prof. Lydie Staron for her helpful comments on an earlier version of this paper.

* manteng@westlake.edu.cn

† heh1@cam.ac.uk

‡ liling@westlake.edu.cn

§ s.torres@westlake.edu.cn

- [1] G. D. R. MiDi, On dense granular flows, *Euro Phys J E* **14**, 341 (2004).
- [2] P. Jop, Y. Forterre, and O. Pouliquen, A constitutive law for dense granular flows, *Nature* **441**, 727 (2006).
- [3] M. Trulsson, B. Andreotti, and P. Claudin, Transition from the viscous to inertial regime in dense suspensions, *Phys Rev Lett* **109**, 118305 (2012).
- [4] T. Man, Q. Feng, and K. Hill, Rheology of thickly-coated granular-fluid systems, *arXiv preprint arXiv:1812.07083* (2018).
- [5] O. Pouliquen, C. Cassar, P. Jop, Y. Forterre, and M. Nicolas, Flow of dense granular material: towards

- simple constitutive laws, *J Stat Mech-Theory E* **2006**, P07020 (2006).
- [6] C. Cassar, M. Nicolas, and O. Pouliquen, Submarine granular flows down inclined planes, *Phys Fluids* **17**, 103301 (2005).
 - [7] G. Lube, H. E. Huppert, R. S. J. Sparks, and A. Freundt, Collapses of two-dimensional granular columns, *Phys Rev E* **72**, 041301 (2005).
 - [8] P.-Y. Lagrée, L. Staron, and S. Popinet, The granular column collapse as a continuum: validity of a two-dimensional navier–stokes model with a μ (i)-rheology, *J Fluid Mech* **686**, 378 (2011).
 - [9] L. Staron and E. Hinch, The spreading of a granular mass: role of grain properties and initial conditions, *Gran Matt* **9**, 205 (2007).
 - [10] L. Rondon, O. Pouliquen, and P. Aussillous, Granular collapse in a fluid: role of the initial volume fraction, *Phys Fluids* **23**, 073301 (2011).
 - [11] L. Staron and E. Hinch, Study of the collapse of granular columns using two-dimensional discrete-grain simulation, *J Fluid Mech* **545**, 1 (2005).
 - [12] X. Zhang, K. Krabbenhoft, and D. Sheng, Particle finite element analysis of the granular column collapse problem, *Gran Matt* **16**, 609 (2014).
 - [13] G. Lube, H. E. Huppert, R. S. J. Sparks, and M. A. Hallworth, Axisymmetric collapses of granular columns, *J Fluid Mech* **508**, 175 (2004).
 - [14] E. Lajeunesse, J. Monnier, and G. Homsy, Granular slumping on a horizontal surface, *Phys Fluids* **17**, 103302 (2005).
 - [15] J. Warnett, P. Denissenko, P. Thomas, E. Kiraci, and M. Williams, Scalings of axisymmetric granular column collapse, *Gran Matt* **16**, 115 (2014).
 - [16] E. Kermani, T. Qiu, and T. Li, Simulation of collapse of granular columns using the discrete element method, *Int J Geomech* **15**, 04015004 (2015).
 - [17] L. Lacaze and R. R. Kerswell, Axisymmetric granular collapse: a transient 3d flow test of viscoplasticity, *Phys Rev Lett* **102**, 108305 (2009).
 - [18] C. M. Mast, P. Arduino, P. Mackenzie-Helnwein, and G. R. Miller, Simulating granular column collapse using the material point method, *Acta Geotec* **10**, 101 (2015).
 - [19] E. J. Fern and K. Soga, The role of constitutive models in mpm simulations of granular column collapses, *Acta Geotec* **11**, 659 (2016).
 - [20] S. Galindo-Torres and D. Pedroso, Molecular dynamics simulations of complex-shaped particles using voronoi-based spheropolyhedra, *Phys Rev E* **81**, 061303 (2010).
 - [21] R. A. Bagnold, Experiments on a gravity-free dispersion of large solid spheres in a newtonian fluid under shear, *P Roy Soc Lond A Mat* **225**, 49 (1954).
 - [22] K. M. Hill and B. Yohannes, Rheology of dense granular mixtures: Boundary pressures, *Phys Rev Lett* **106**, 058302 (2011).